Effects of low reactivity fuel characteristics and blending ratio on low load RCCI (reactivity controlled compression ignition) performance and emissions in a heavy-duty diesel engine

Energy, Volume 90, October 2015, Pages 1261-1271. http://dx.doi.org/10.1016/j.energy.2015.06.088

Jesús Benajes, Santiago Molina, Antonio García* and Javier Monsalve-Serrano

CMT - Motores Térmicos, Universitat Politècnica de València, Camino de Vera s/n, 46022 Valencia, Spain

(*) Corresponding author: angarma8@mot.upv.es (Antonio García Martínez)

Abstract

This work investigates the effect of low reactivity fuel characteristics and blending ratio on low load RCCI performance and emissions using four different low reactivity fuels: E10-95, E10-98, E20-95 and E85 (port fuel injected) while keeping constant the same high reactivity fuel: diesel B7 (direct injected). The experiments were conducted using a heavy-duty single-cylinder research diesel engine adapted for dual fuel operation. All tests were carried out at 1200 rev/min and constant CA50 of 5 CAD ATDC. For this purpose, the premixed energy was equal for the different blends and the EGR rate was modified as required, keeping constant the rest of engine settings. In addition, a detailed analysis of air/fuel mixing process has been developed by means of a 1-D spray model.

Results suggest that in-cylinder fuel reactivity gradients strongly affect the engine efficiency at low load. Specifically, a reduced reactivity gradient allows an improvement of 4.5% in terms of gross indicated efficiency when the proper blending ratio is used. In addition, EURO VI NOx and soot emission levels are fulfilled with a strong reduction in CO and HC compared with the case of the higher reactivity gradient among the low and high reactivity fuel.

Keywords

Reactivity Controlled Compression Ignition; Low load; Low reactivity fuels; mixing process; Efficiency

1. Introduction

As response of the regulations introduced around the world to limit the pollutant emissions associated to internal combustion engines, researchers and manufacturers are focusing their effort on develop new combustion strategies and aftertreatment systems to fulfill the stringent limitations. Since the complex aftertreatment devices incur in higher costs and fuel consumption, the in-cylinder emissions reduction is clearly necessary.

Homogeneous charge compression ignition (HCCI) is a widely investigated LTC combustion concept. It has been demonstrated its potential to produce virtually no soot or NOx emissions while maintaining high efficiency [1][2][3], but in return, new challenges regarding combustion control [4][5] and mechanical engine stress were also identified [6]. Thus, Bessonette et al. [7] suggested that different in-cylinder reactivity is required for proper HCCI operation under different operating conditions. In particular, high cetane fuels are required at low load and a low cetane fuels are needed at medium-high load. With the aim of improving the reduced controllability and excessive knocking in HCCI combustion, the use of gasoline-like fuels under partially premixed combustion (PPC) strategies has been widely studied [8-12]. The investigations confirmed gasoline PPC as promising method to control the heat release rate while providing a simultaneous reduction in NOx and soot emissions [13][14]. However, the concept demonstrated difficulties at low load conditions using gasoline with octane number (ON) greater than 90 [15][16]. In this sense, the spark assistance provided temporal and spatial control over the gasoline PPC combustion process [17][18][19], but resulted in unacceptable NOx and soot emissions [20], even using double injection strategies [21][22].

Recent trends in LTC investigation confirm the extensive interest of the research community in dual-fuel compression ignition combustion. This combustion mode enables an effective control of the in-cylinder equivalence ratio and reactivity stratification, which allows a flexible operation over a wide operating range. Experimental and simulated studies proved that reactivity controlled compression ignition (RCCI), a dual-fuel diesel-gasoline combustion concept, is a more promising LTC technique than HCCI and PPC [23][24]. Thus, several investigations have been conducted with the aim of insight into the RCCI phenomena. First of all, the effects of the gasoline percentage in the blend and direct injection timing were widely studied [25][26][27]. These works revealed that RCCI concept allows to reach ultra-low NOx and soot emissions levels, together with improved fuel consumption compared to conventional diesel combustion (CDC). In this direction, further investigations confirmed the potential of combining different engine settings, such as in-cylinder gas temperature and oxygen concentration with the fuel blending ratio, to improve the RCCI low load combustion efficiency to values above 98% [28]. Finally, the influence of geometric factors such as compression ratio and piston geometry on RCCI emissions have been also investigated [29]. In this sense, crevices and squish volumes were identified as primary responsible of incomplete combustion. In addition, it was also identified that RCCI concept offers an interesting potential for improving fuel consumption by lowering wall heat transfer [24].

Taking into account the major findings about RCCI described above, it is clear that local reactivity plays a fundamental role to enhance the RCCI combustion propagation, which proceed gradually from high reactivity to low reactivity regions, reducing the incomplete combustion. In this sense, a primary source of local reactivity in RCCI concept is the in-cylinder fuel blending, which can be managed as required depending on the engine operating conditions. Thus, several studies confirm that in order to achieve high efficiency while reducing NOx and soot emissions, the higher portion of the energy should come from the low reactivity fuel. Taking into account this statement, it is clear that the low reactivity fuel characteristics and its amount in the blend have a significant contribution to the in-cylinder reactivity. Thus, the main objective of the present work is to evaluate the effect of the low reactivity fuel characteristics and blending ratio on RCCI combustion efficiency as well as on its performance and emissions at low load. For this purpose, four different low reactivity fuels (port fuel injected) were tested keeping constant the same high reactivity fuel. In order to provide details in terms of combustion development, emissions and efficiency differences between the different fuel blends, the experiments were conducted at constant combustion phasing (CA50).

2. Experimental Facilities and Processing Tools

2.1. Test cell and engine description

A single-cylinder, heavy-duty (HD) diesel engine representative of commercial truck engine, has been used for all experiments in this study. The major difference to the standard unit production is the hydraulic VVA system, which confers great flexibility during the research. In particular, the valve timing, duration and lift can be electronically controlled for each valve during the engine tests. Thus, a slightly adapted cylinder head to include a dedicated oil circuit is required. Detailed specifications of the engine are given in Table 1.

As it is illustrated in Figure 1, the engine was installed in a fully instrumented test cell, with all the auxiliary facilities required for its operation and control. In addition, Table 2 summarizes the accuracy of the instrumentation used in this work.

Moreover, to achieve stable intake air conditions, a screw compressor supplied the required boost pressure before passing through an air dryer. The air pressure was adjusted within the intake settling chamber, while the intake temperature was controlled in the intake manifold after mixing with the exhaust gas recirculation (EGR) flow. The exhaust backpressure produced by the turbine in the real engine was replicated by means of a valve placed in the exhaust system, controlling the pressure in the exhaust settling chamber. Low pressure EGR was produced taking exhaust gases from the exhaust settling chamber. Thus, the determination of the EGR rate was carried out using the experimental measurement of intake and exhaust CO_2

concentration. The concentrations of NOx, CO, unburned HC, intake and exhaust CO_2, and O_2 were analyzed with a five gas Horiba MEXA-7100 DEGR analyzer bench by averaging 40 seconds after attaining steady state operation. Smoke emission were measured with an AVL 415S Smoke Meter and averaged between three samples of a 1 liter volume each with paper-saving mode off, providing results directly in FSN (Filter Smoke Number) units. PM measurements of FSN were transformed into specific emissions (g/kWh) by means of the factory AVL calibration.

2.2. Fuels and delivery

To enable RCCI operation the engine was equipped with a double injection system, one for each different fuel used. This injection hardware enables to vary the in-cylinder fuel blending ratio and fuel mixture properties according to the engine operating conditions. Thus, to inject the diesel fuel, the engine was equipped with a common-rail flexible injection hardware which is able to perform up to five injections per cycle. The main characteristic of this hardware is its capability to amplify common-rail fuel pressure for one of the injection events by means of a hydraulic piston directly installed inside the injector. Concerning the gasoline injection, an additional fuel circuit was in-house built including a reservoir, fuel filter, fuel meter, electrically driven pump, heat exchanger and commercially available port fuel injector (PFI). The mentioned injector was located at the intake manifold and was specified to be able to place all the gasoline fuel into the cylinder during the intake stroke. Consequently, the gasoline injection timing was fixed 10 CAD after the IVO to allow the fuel to flow along 160 mm length (distance from PFI location to intake valves seats). Accordingly, this set-up avoids fuel pooling over the intake valve and the undesirable variability introduced by this phenomenon. The main characteristics of the diesel and gasoline injectors are depicted in Table 3.

To carry out the experimental tests, commercially available diesel and four different low reactivity fuels were used. Their main properties related with auto-ignition are listed in Table 4. All the properties were obtained following ASTM standards.

2.3. Analysis of in-cylinder pressure signal

The combustion analysis was performed with an in-house one-zone model named CALMEC, which is fully described in [30]. This combustion diagnosis tool uses the in-cylinder pressure signal and some mean variables (engine speed, coolant, oil, inlet and exhaust temperatures, air, EGR and fuel mass flow…) as its main inputs.

The pressure traces from 150 consecutive engine cycles were recorded in order to compensate the cycle-to-cycle variation during engine operation. Thus, each individual cycle's pressure data was smoothed using a Fourier series low-pass filter. Once filtered, the collected cycles were ensemble averaged to yield a representative cylinder pressure trace, which was used to perform the analysis. Then, the first law of thermodynamics was applied between intake valve closing (IVC) and exhaust valve opening (EVO), considering the combustion chamber as an open system because of the blow-by and fuel injection. The ideal gas equation of state was used to calculate the mean gas temperature in the chamber. In addition, the in-cylinder pressure signal allowed obtaining the gas thermodynamic conditions in the chamber to feed the convective and radiative heat transfer models in the chamber [31], as well as the filling and emptying model that provided the fluid-dynamic conditions in the ports, and thus the heat transfer flows in these elements. The convective and radiative models are linked to a lumped conductance model to calculate the wall temperatures.

The main results of the model used in this work were the Rate of Heat Release (RoHR) as well as the heat transfer analysis. Moreover, several parameters were calculated from the RoHR profile. In particular, start of combustion (defined as the crank angle position in which the cumulated heat release has reached 2%), end of combustion (defined as the crank angle position in which the cumulated heat release has reached 90%) and combustion phasing (defined as the crank angle position of 50% fuel mass fraction burned) were obtained. Additionally, ringing intensity was calculated by means of the correlation of Eng [32]:

$$\mathrm{RI} = \frac{1}{2\gamma}\frac{[0.05 \cdot (\mathrm{dP/dt})_{\mathrm{max}}]^2}{\mathrm{P_{max}}}\sqrt{\gamma \mathrm{RT_{max}}}$$

(1)

Where γ is the ratio of specific heats, $(dP/dt)_{max}$ is the peak PRR, P_{max} is the maximum of in-cylinder pressure, R is the ideal gas constant, and T_{max} is the maximum of in-cylinder temperature.

2.4. Analysis of mixing process

A 1-D spray model, DICOM [33][34], has been used to understand the changes in mixing process associated to variations in the in-cylinder fuel blending and intake oxygen concentration. The necessary inputs for the model are the evolution of the in-cylinder thermodynamic conditions (pressure, temperature and density), the spray cone angle and the fuel mass injection rate. To reproduce the real in-cylinder conditions more accurately, two additional inputs are also needed for the 1-D model; the oxygen mass fraction at IVC and the stoichiometric equivalence ratio of the in-cylinder fuel blend (2) [35]. These two parameters are used to account the fresh air, EGR rate and low reactivity fuel entrainment. Finally, the calculation time for each test was set from the start of injection of HRF (SOI_{HRF}) to the experimental start of combustion (SOC).

$$\phi_{est} = \frac{1-\phi_{LRF}}{C_{HRF}+\frac{H_{HRF}}{4}-\frac{O_{HRF}}{2}} \cdot \frac{12\,C_{HRF}+H_{HRF}+16\,O_{HRF}}{32} \cdot \frac{1}{1+\frac{Y_{N2,IVC}}{Y_{O2,IVC}}+\phi_{LRF}\cdot\frac{1}{C_{LRF}+\frac{H_{LRF}}{4}-\frac{O_{LRF}}{2}}\cdot\frac{12\,C_{LRF}+H_{LRF}+16\,O_{LRF}}{32}}$$

(2)

Where ϕ_{LRF} and ϕ_{HRF} are the equivalence ratios of low reactivity fuel (LRF) and high reactivity fuel (HRF), C_{HRF} and C_{LRF} denote the number of carbon atoms, H_{HRF} and H_{LRF} are the number of hydrogen atoms, $Y_{N2,IVC}$ stands for nitrogen mass fraction at IVC and $Y_{O2,IVC}$ accounts the oxygen mass fraction at IVC.

To perform the calculations, the model solves the general conservation equations either in a transient or steady formulation for axial momentum and fuel mass in terms of the on-axis (i.e., center line) referred to instantaneous values of velocity and species mass fractions. Finally, by processing the raw results, the high reactivity fuel mass distribution mixed to different equivalence ratios at experimental SOC was obtained. Figure 3 shows an example of the 1-D model results as a histogram. In this case, the bars represent the result of the high reactivity fuel masses mixed to different local equivalence ratios and the solid line represents the envelope curve of the bars. For the sake of clarity, in the present work the results were also represented as a pie chart format.

3. Test methodology

As literature demonstrates, to achieve high efficiencies in a wide range of engine speeds and loads during RCCI operation, the mass ratio of premixed fuel (low reactivity) to direct injected fuel (high reactivity) should be changed accordingly. Previous works defined the in-cylinder fuel blending ratio as the mass of premixed fuel to the total fuel. However, since there is a significant difference in lower heating value (LHV) between E85 and the three remaining low reactivity fuels tested, as shown in Table 4, the premixed energy ratio (PER) is presented here. Thus, the premixed energy ratio is defined as the ratio of energy of the low reactivity fuel to the total fuel (3), where the low reactivity fuel and the high reactivity one are denoted by the subscripts LRF and HRF respectively.

$$PER[\%] = \frac{m_{LRF} \cdot LHV_{LRF}}{m_{HRF} \cdot LHV_{HRF} + m_{LRF} \cdot LHV_{LRF}}$$

(3)

In the present study, four different premixed energy ratios were tested for each fuel blend. The baseline operation was selected according to B7+E20-95 blend. In this sense, four different blending ratios were proposed (mass based) and then, the total energy delivered to the cylinder was maintained constant for the three remaining blends by adjusting the low reactivity fuel mass as required in each case. The diesel B7 mass was kept constant for each premixed energy ratio between the different fuel blends. In order to clarify the test methodology, Table 5 depicts the fuel mass per blend as well as the total energy delivered to the cylinder for each PER proposed.

All the tests were carried out at 1200 rev/min and constant combustion phasing (CA50) of 5 CAD ATDC. In order to keep constant the CA50 while introducing low reactivity fuels with very different characteristics, the EGR rate was modified as required in each case, keeping constant the rest of engine settings. At these operating conditions, the mean IMEP resulted in 7.5 bar, with a maximum value of 7.83 bar (E10-95 and PER 59%) and minimum value of 7.03 bar (E10-95 and PER 59%) due to differences in combustion development between fuels. Table 6 depicts the constant engine settings.

4. Results and discussion

4.1. Combustion development

In order to understand the main differences in combustion process due to variations in low reactivity fuel characteristics, an analysis of the parameters derived from the in-cylinder pressure measurement is presented here. In this sense, the instantaneous RoHR traces for the different premixed energy ratios and blends are shown in Figure 4. A detailed view of the low temperature heat release (LTHR) profiles is presented inside each figure. In addition, the EGR rate, combustion duration (CA90-CA10) and ringing intensity are depicted in Figure 5, Figure 7 and Figure 8, respectively. It is interesting to note that, in the case PER=79% was not possible to obtain the desired combustion phasing (5 CAD ATDC) with E85, even without the use of EGR. In this case, the higher octane number of ethanol E85 combined with the greater intake cooling effect associated to its significantly higher enthalpy of vaporization compared with the conventional gasolines [36][37][38], delayed the combustion far from 5 CAD ATDC.

As explained in the test methodology, in order to keep constant the CA50 while introducing low reactivity fuels with very different characteristics, the EGR rate was modified as required in each case. Thus, Figure 5 shows the EGR rate for the different premixed energy ratios and blends. As expected, the results illustrate that the EGR rate depends on the blend reactivity. Taking into account that diesel injection timing as well as its injected fuel mass was kept constant for each PER, the blend reactivity was modified only by means of the low reactivity fuel. Focusing on the values depicted in Table 4, it is clear that the higher RON and MON, the lower EGR rate needed to maintain the combustion phasing. Moreover, as PER is increased, a deterioration in the blend reactivity is promoted due to the low diesel fuel mass, requiring lower EGR rates for the same blend.

In RCCI operation, the combustion starts with the autoignition of the high reactivity fuel followed by the entrained low reactivity fuel. The consequent increase in temperature and pressure initiates a reaction zone, identified in literature as an auto-ignition or flame propagation depending on equivalence ratio conditions, which proceed gradually from high to low reactivity regions of the combustion chamber [39][40][41]. Focusing on the RoHR profiles in Figure 4, it is clear that the SOC pattern of the high temperature heat release (HTHR) stages between the different fuels is the same independently on PER. In particular, B7+E85 exhibits earlier HTHR growth, followed by B7+E10-98, B7+E20-95 and finally B7+E10-95. Considering the low reactivity fuel characteristics, it is clear that this pattern is opposite to the fuel blend reactivity (i.e., octane number). In this sense, the increase in oxygen concentration through the EGR reduction counteracts the deterioration in the mixture reactivity due to the fuel characteristics. Thus, an earlier HTHR growth is achieved in spite of the high ON fuel blend [42]. In addition, the higher oxygen content of E85 compared to other fuels also contributes to the more evident advance in the HTHR onset.

Figure 6 illustrate some pie charts of the high reactivity fuel mass distribution mixed to different ϕ at experimental SOC for the different premixed energy ratios and blends. From the four scenarios proposed, the ones containing the more reactive equivalence ratios ($0.9<\phi<1.1$) govern the autoignition process. In this sense, it is possible to see how there is not a significant difference in the mass distribution for the diesel fuel when comparing the cases of B7+E20-95, B7+E10-98 and B7+E10-95, whatever the PER. Thus, the first slope in the HTHR profiles for these three blends are nearly equal. Regarding the diesel mass distribution in the case of E85 for these two ranges of equivalence ratios, it is shown that in the cases of PER=49% and PER=59% the fuel mass distribution is very similar to the ones obtained with the other three blends. However, the EGR rate reduction needed in the case of PER=69% to kept constant the combustion phasing promotes a very lean mixture distribution, leading to an only 0.5% fuel mass mixed in the ϕ range of $0.9<\phi<1.1$ and no fuel mass mixed to $\phi>1.1$. From the figure, it is highlighted that the diesel fuel mass distribution becomes leaner as PER is increased, whatever the fuel blend. This behavior is explained due to the low diesel fuel mass injected and the greater fresh air amount (lower EGR) provided to the cylinder. This fact, combined with the stoichiometric equivalence ratio of the low reactivity fuel, contributes to determinate the amount of diesel fuel mass mixed to the leanest ϕ range ($0.1<\phi<0.5$). The over-lean diesel fuel stratification will cause a deterioration in the combustion propagation. As it is noted from the figure, the same pattern in terms of diesel amount mixed to this ϕ range is appreciated (E85>E20-95>E10-98>E10-95), whatever the PER.

Once initiated the combustion, its evolution strongly depends on the low reactivity fuel characteristics and the high reactivity fuel stratification. Figure 7 shows the combustion duration (CA90-CA10) for the different PER and blends. Once again, the combustion duration trend is well correlated with the fuel blend reactivity. In this sense, the low reactivity fuels with higher reactivity enhance the autoignition process, which results in higher maximum RoHR peaks during the HTHR stage and shorter combustion durations. Another interesting finding from the RoHR profiles in Figure 4 is that the late combustion phase, from +10 to +20 CAD ATDC, is almost equal whatever the PER and blend. Hence, the end of combustion (EOC) is almost the same between fuels for the same PER.

Regarding LTHR profiles, in previous work [28] in which an analysis of the temporal evolution of the key combustion species was presented, it was demonstrated that the low temperature reactions are mainly associated to the high reactivity fuel. The low temperature reactions are triggered by the high reactivity fuel consumption. However, since the low reactivity fuel is well mixed at this moment, the temperature increase makes the surrounding zones start also to react. Focusing on the evolution of the LTHR profiles represented in the detailed views in Figure 4, it is clear that the maximum LTHR peak becomes reduced as PER is increased, whatever the low reactivity fuel used. In addition, it is stated that for the same PER, the maximum LTHR peak depends on the reactivity of the low reactivity fuel. Thus, the maximum LTHR peak is well related to the octane number of the low reactivity fuels, with higher LTHR peaks observed as the RON and MON are decreased.

Finally, from Figure 8, it is stated that ringing intensity trends between the different blends are the same regardless the PER. Hence, RI is directly related to the blend reactivity. Since the diesel fuel mass was kept constant for each PER, the blend reactivity is modified only by means of the LRF. Focusing on the values depicted in Table 4, it is clear that the higher RON and MON, the lower RI registered. Also it is interesting that RI values for each fuel become lower as PER is increased. Thus, slightly higher RI values are obtained with the lower PER due to the enhancement in the blend reactivity through the higher diesel fuel mass. It is remarkable that

RI values are below 5 MW/m^2, which was established by Dec and Yang [43] as a proper upper limit to achieve an acceptable combustion noise and knock-free operation.

4.2. NOx emissions

Figure 9 represents the NOx emissions for the different premixed energy ratios and blends**.** As reference, dashed lines across the figures denote the EURO VI NOx limits for HD diesel engines according to the world harmonized stationary cycle (WHSC), which stablishes a maximum value of 0.4 g/kWh for NOx emissions.

From the figure it is noted that E85 leads to significantly higher NOx emission levels than the other low reactivity fuels since much lower EGR rate (Figure 5) is required to maintain the proper combustion phasing. The EGR rate reduction promotes an increase in combustion temperature, represented in Figure 10. This higher temperature achieved during the combustion development enhances the NO formation reactions promoting an increase in the NOx levels. Also of note is that as PER is increased, NOx emissions increase whatever the blend. In this case, a reduction in the EGR rate is necessary to keep constant the CA50 while reducing the diesel fuel mass. It is interesting to note that E20-95, E10-98 and E10-95 are valid to fulfill EURO VI NOx limits independently on the PER. Specifically, the higher reactivity of E10-95 allows to use higher EGR rates, leading to emission levels far below of the current regulation limits.

4.3. Soot emissions

Soot emissions were measured for the different premixed energy ratios and blends. The soot levels registered were below the minimum detection limit of the AVL 415S Smoke Meter in all tests. Thus, under this operating conditions, engine-out soot emissions from RCCI operation are zero whatever the low reactivity fuel used. Consequently, the limitation in PM mass established by the EURO VI regulation for HD diesel engines referred to the WHSC (0.01 g/kWh), is also fulfilled.

The results confirm that RCCI soot emissions are mainly associated to the soot formation and oxidation processes from the high reactivity fuel. In this sense, an advanced enough injection strategy for the direct injected fuel is required to provide sufficient mixing time prior to the start of combustion and inhibit soot formation. Concerning the specific injection timing values used in this research, shown in Table 6, the pilot direct injection timing was set at -60 CAD ATDC in order to ensure that part of the high reactivity fuel mass had sufficient mixing time prior to the start of combustion. Moreover, it is interesting to note that the value selected for the main injection (-30 CAD ATDC) is advanced enough to allow an adequate mixing time for this second fuel mass too, achieving soot levels below the minimum detection limit of the AVL 415S Smoke Meter in all tests. In order to confirm that the strategy to achieve zero soot is to avoid its formation, Figure 11 presents the mass distribution mixed up to different equivalence ratios at experimental SOC for the diesel fuel calculated by means of the 1-D spray model (DICOM). The different PER and blends are also depicted in the figure. As it can be seen, the higher maximum local equivalence ratios are obtained for the lowest PER as a result of the higher diesel amount injected in these cases. Even in these conditions, the value of the maximum local equivalence ratio is around $\phi_L=2$, which confirm the non-formation of soot [44][45][46]. Moreover, it is interesting to remark how an E85/air ambient enhances the mixing process for the diesel fuel.

4.4. HC and CO emissions

Figure 12 and Figure 13 represent HC and CO emissions for the different premixed energy ratios and blends, respectively. Dashed lines across the figures denote the EURO VI HC and CO limits for HD diesel engines according to the WHSC approval cycle (HC <0.13 g/kWh and CO <1.5 g/kWh).

Taking into account the maximum RoHR peaks in Figure 6, it is demonstrated that the low cylinder reactivity gradients enhance the autoignition process. From Figure 12 it is noted that unburned HC emissions correlate with the fuel blend reactivity, which is also related with the maximum energy released during the combustion. Specifically, as the fuel blend reactivity is increased (i.e., lower ON) higher RoHR peaks (Figure 6) and lower unburned HC are registered. This behavior is the same whatever the PER tested.

Regarding CO emissions, a reduction in its emission levels are achieved as PER is increased from 49% to 69% for all the blends. This trend is explained due to the higher combustion temperatures (Figure 10) attained (promoted by the EGR rate reduction required), which improves the oxidation process. Increasing the PER up to 79%, it is possible to appreciate a rise in the CO levels for the three blends. At this point, the deterioration in the combustion process (larger combustion duration and lower RoHR peaks) promoted by the over-lean in-cylinder regions, results in higher CO levels even with higher in-cylinder temperature peaks.

The results suggests that, that independently on the PER, a reduced reactivity gradient between the low and high reactivity fuel enhances the combustion propagation, reducing the unburned HC and CO emission levels. However, independently on PER and fuel blend, unacceptable limits are obtained taking into account the EURO VI limits. In this sense, recent study discussed the effectiveness of several diesel oxidation catalyst (DOC) with different precious metal loadings under steady-state operation [47]. It was demonstrated that all DOCs were effective in oxidizing CO and HC at temperatures greater than 300 °C, with no catalyst activity under 200 °C.

4.5. Discussion

This section is focused on detailing the influence of the different combinations of fuels and blending ratios on RCCI concept efficiency. For this purpose, Figure 14 represents the gross indicated efficiency (GIE), heat transfer losses, exhaust losses and combustion losses as a percentage of the fuel energy for the different premixed energy ratios and blends.

The results illustrate that, at low load, the gross indicated efficiency of RCCI operation using E85 as low reactivity fuel is considerably lower than the ones obtained using the other low reactivity fuels tested. Taking into account the energy distribution, it is clear that the main cause of the differences in GIE are related to the differences in combustion losses. In this case, the higher unburned HC and CO levels (which leads to incomplete combustion) prevails over the reduction in heat transfer and exhaust losses, which results in the GIE reduction. The combination of B7+E10-95 allows an improvement between 3 and 4.5% in terms of GIE in comparison with B7+E85. Thus, it is demonstrated that, at low load, a reduced reactivity gradient between the low and high reactivity fuel is needed to improve the thermal efficiency.

Comparing the results between B7+E20-95, B7+E10-98 and B7+E10-95, in which the combustion temperatures are similar as well as the combustion development, it is appreciated that the gross indicated efficiency is also mainly correlated with the combustion efficiency. Moreover, the higher GIE for B7+E10-95 is also related with its higher maximum RoHR peaks and shorter combustion durations whatever the PER.

5. Conclusions

The present study focused on evaluating the influence of the low reactivity fuel characteristics and blending ratio on RCCI combustion efficiency, performance and emissions at low load. In particular, an analysis of the parameters derived from in-cylinder pressure signal has been combined with a detailed air/fuel mixing process analysis. The major findings from the combustion development study are summarized as follows:

- The maximum LTHR peak became reduced as PER increased, whatever the low reactivity fuel used. At same PER, the maximum LTHR peak was dependent also on the reactivity of the low reactivity fuel.
- The greater intake oxygen concentration (lower EGR rate) plus the higher oxygen content of E85 fuel compared to other fuels, resulted in advanced HTHR growth. In addition, the HTHR onset pattern for the remaining fuels was clearly related to the EGR rate.
- The combustion development was strongly affected by the low reactivity fuel characteristics. Thus, the low reactivity fuels with higher reactivity enhanced the autoignition process shortening the combustion duration.
- Knock-free operation was achieved for any fuel blend. In addition, it was demonstrated that the higher RON and MON of the low reactivity fuel, the lower ringing intensity registered.

The notable observations comparing performance and emissions from the different combinations of high and low reactivity fuel were as follows:

- The low EGR rate required with E85 fuel enhanced the thermal NOx formation resulting in emissions levels far above the EURO VI legislation limit.
- Independently on the low reactivity fuel used, soot formation was inhibited by setting an advanced injection strategy for the diesel fuel.
- The reduced reactivity gradient between high and low reactivity fuels enhanced the combustion propagation, which allowed a considerable reduction in HC and CO emissions. The decrease in combustion losses counteracted the increase in heat transfer and exhaust losses, which resulted in greater GIE in this case.

The results of this work demonstrate that the in-cylinder fuel reactivity gradients strongly affect the engine efficiency at low load. In particular, an improvement of 4.5% in terms of GIE was achieved by reducing the reactivity gradient and selecting the proper blending ratio. In terms of engine-out emissions, the use of a lower in-cylinder reactivity gradient allowed a notable reduction in CO and unburned HC levels. Moreover, EURO VI NOx and soot emission levels are fulfilled in this case. In addition, ringing intensity values are below 5 MW/m^2, which denotes knock-free operation.

Acknowledgments

The authors acknowledge VOLVO Group Trucks Technology and TOTAL for supporting this research.

References

[1]Mingfa Y, Zhaolei Z, Haifeng L. Progress and recent trends in homogeneous charge compression ignition (HCCI) engines. Progress in Energy and Combustion Science 35 (5) (October 2009) 398-437.

[2]Maurya R K, Agarwal A K. Experimental study of combustion and emission characteristics of ethanol fuelled port injected homogeneous charge compression ignition (HCCI) combustion engine. Applied Energy, Vol. 88, pp 1169-1180, 2011.

[3]Lu X, Han D, Huang Z. Fuel design and management for the control of advanced compression-ignition combustion modes. Progress in Energy and Combustion Science, 37, 2011:741-783.

[4]Stanglmaier R, Roberts C. Homogeneous Charge Compression Ignition (HCCI): Benefits, Compromises, and Future Engine Applications. SAE Technical Paper 1999-01-3682, 1999, doi:10.4271/1999-01-3682.

[5]Tanaka S, Ayala F, Keck J, Heywood J. Two-stage ignition in HCCI combustion and HCCI control by fuels and additives. Combustion and Flame 132 (2003) 219–239.

[6]Cerit M, Soyhan H S. Thermal analysis of a combustion chamber surrounded by deposits in an HCCI engine. Applied Thermal Engineering 50 (1) (2013) 81-88.

[7]Bessonette P W, Schleyer C H, Duffy K P, Hardy W L, Liechty M P. Effects of fuel property changes on heavy-duty HCCI combustion. SAE paper 2007-01-0191, 2007.

[8]Lewander C M, Johansson B, Tunestal P. Extending the Operating Region of Multi-Cylinder Partially Premixed Combustion using High Octane Number Fuel. SAE Paper 2011-01-1394; 2011.

[9]Kalghatgi G, Risberg P, Ångström H. Partially Pre-Mixed Auto-Ignition of Gasoline to Attain Low Smoke and Low NOx at High Load in a Compression Ignition Engine and Comparison with a Diesel Fuel. SAE Technical Paper 2007-01-0006, 2007, doi:10.4271/2007-01-0006.

[10]Hanson R, Splitter D, Reitz R. Operating a Heavy-Duty Direct-Injection Compression-Ignition Engine with Gasoline for Low Emissions. SAE Technical Paper 2009-01-1442, 2009, doi:10.4271/2009-01-1442.

[11]Payri R, García A, Domenech V, Durrett R, Plazas A. An experimental study of gasoline effects on injection rate, momentum flux and spray characteristics using a common rail diesel injection system. Fuel, Volume 97, July 2012, Pages 390–399.

[12]López JJ, García-Oliver JM, García A, Domenech V. Gasoline effects on spray characteristics, mixing and auto-ignition processes in a CI engine under Partially Premixed Combustion conditions. Applied Thermal Engineering, Volume 70, Issue 1, 5 September 2014, Pages 996–1006.

[13]Kalghatgi G T. Auto-ignition quality of practical fuels and implications for fuel requirements of future SI and HCCI engines. SAE paper 2005-01-0239, 2005.

[14]Kalghatgi G, Risberg P, Angstrom H. Advantages of fuels with high resistance to autoignition in late-injection, low-temperature, compression ignition combustion. SAE Trans., 2006, 115(4), 623–634.

[15]Liu H, Yao M, Zhang B, Zheng Z. Effects of inlet pressure and octane numbers on combustion and emissions of a homogeneous charge compression ignition (HCCI) engine. Energy and Fuels, 2008, 22(4), 2207–2215.

[16]Christensen M, Hultqvist A, Johansson B. Demonstrating the multi-fuel capability of a homogeneous charge compression ignition engine with variable compression ratio. SAE paper 1999-01-3679, 1999.

[17]Benajes J, García A, Domenech V, Durrett R. An investigation of partially premixed compression ignition combustion using gasoline and spark assistance. Applied Thermal Engineering, Volume 52, Issue 2, 15 April 2013, Pages 468-477.

[18]Benajes J, García A, Tormos B, Monsalve-Serrano J. Impact of Spark Assistance and Multiple Injections on Gasoline PPC Light Load. SAE Int. J. Engines 7(4):2014, doi:10.4271/2014-01-2669.

[19] Pastor JV, García-Oliver JM, García A, Micó C, Durrett R. A spectroscopy study of gasoline partially 365 premixed compression ignition spark assisted combustion. Appl Energy 2013;104:568–75. 366.

[20]Desantes JM, Payri R, García A, Monsalve Serrano J. Evaluation of Emissions and Performances from Partially Premixed Compression Ignition Combustion using Gasoline and Spark Assistance. SAE Technical Paper 2013-01-1664, 2013, doi:10.4271/2013-01-1664.

[21]Benajes J, Molina S, García A, Monsalve-Serrano J, Durrett R. Conceptual model description of the double injection strategy applied to the gasoline partially premixed compression ignition

combustion concept with spark assistance. Applied Energy, Volume 129, 15 September 2014, Pages 1-9.

[22]Benajes J, Molina S, García A, Monsalve-Serrano J, Durrett R. Performance and engine-out emissions evaluation of the double injection strategy applied to the gasoline partially premixed compression ignition spark assisted combustion concept. Applied Energy, Volume 134, 1 December 2014, Pages 90-101.

[23]Splitter D A, Wissink M L, Hendricks T L, Ghandhi J B, Reitz R D. Comparison of RCCI, HCCI, and CDC Operation from Low to Full Load, THIESEL 2012 Conference on Thermo- and Fluid Dynamic Processes in Direct Injection Engines, 2012.

[24]Kokjohn S L, Hanson R M, Splitter D A, Reitz R D. Fuel reactivity controlled compression ignition (RCCI): a pathway to controlled high-efficiency clean combustion, International Journal of Engine Research, 2011. Volume 12, June 2011, Pages 209-226.

[25] Li J, Yang W M, An H, Zhou D Z, Yu W B, Wang J X, Li L. Numerical investigation on the effect of reactivity gradient in an RCCI engine fueled with gasoline and diesel. Energy Conversion and Management, Volume 92, 1 March 2015, Pages 342-352.

[26] Splitter D, Hanson R, Kokjohn S, Wissink M, et al. Injection Effects in Low Load RCCI Dual-Fuel Combustion. SAE Technical Paper 2011-24-0047, 2011, doi:10.4271/2011-24-0047.

[27]Benajes J, Molina S, García A, Monsalve-Serrano J. Effects of Direct injection timing and Blending Ratio on RCCI combustion with different Low Reactivity Fuels. Energy Conversion and Management, Volume 99, 15 July 2015, Pages 193-209.

[28]Desantes J M, Benajes J, García A, Monsalve-Serrano J. The Role of the In-Cylinder Gas Temperature and Oxygen Concentration over Low Load RCCI Combustion Efficiency. Energy, Volume 78, 15 December 2014, Pages 854–868.

[29]Splitter D A, Kokjohn S L, Wissink M L, Reitz R. Effect of compression ratio and piston geometry on RCCI load limits and efficiency. SAE technical paper 2012-01-0383; 2012. http://dx.doi.org/10.4271/2012-01-0383.

[30]Payri F, Olmeda P, Martín J, García A. A complete 0D thermodynamic predictive model for direct injection diesel engines. Applied Energy, Volume 88, Issue 12, December 2011, Pages 4632-4641.

[31]Payri F, Olmeda P, Martin J, Carreño R. A New Tool to Perform Global Energy Balances in DI Diesel Engines. SAE Int. J. Engines 7(1):2014, doi:10.4271/2014-01-0665.

[32]Eng J. Characterization of pressure waves in HCCI combustion. SAE paper 2002-01-2859, 2002.

[33] Arrègle J, López JJ, García JM, Fenollosa C. Development of a zero-dimensional diesel combustion model, part 2: analysis of the transient initial and final diffusion combustion phases. Applied Thermal Engineering, 23 (2003) 1319e1331.

[34] Pastor JV, López JJ, García JM, Pastor JM. A 1D model for the description of mixing-controlled inert diesel sprays. Fuel 87 (2008) 2871e2885.

[35] Benajes J, Molina S, García A, Belarte E, Vanvolsem M. An investigation on RCCI combustion in a heavy duty diesel engine using in-cylinder blending of diesel and gasoline. Applied Thermal Engineering, vol. 63, 66-76, 2014.

[36] Sjoberg M, Dec J. Smoothing HCCI Heat Release with Vaporization-Cooling-Induced Thermal Stratification using Ethanol. SAE Int. J. Fuels Lubr. 5(1):7-27, 2012, doi:10.4271/2011-01-1760.

[37] Foong T, Morganti K, Brear M, da Silva G, et al. The Effect of Charge Cooling on the RON of Ethanol/Gasoline Blends. SAE Int. J. Fuels Lubr. 6(1):34-43, 2013, doi:10.4271/2013-01-0886.

[38] Huang Y, Hong G, Cheng X, Huang R. Investigation to Charge Cooling Effect of Evaporation of Ethanol Fuel Directly Injected in a Gasoline Port Injection Engine. SAE Technical Paper 2013-01-2610, 2013, doi:10.4271/2013-01-2610.

[39] Kokjohn S, Reitz R, Splitter D, Musculus M. Investigation of Fuel Reactivity Stratification for Controlling PCI Heat-Release Rates Using High-Speed Chemiluminescence Imaging and Fuel Tracer Fluorescence. SAE Int.J. Engines 5(2):2012, doi:10.4271/2012-01-0375.

[40] Dronniou N. Kashdan J. Lecointe B. Sauve K, et al. Optical Investigation of Dual-fuel CNG/Diesel Combustion Strategies to Reduce CO2 Emissions. SAE Int. J. Engines 7(2):2014, doi:10.4271/2014-01-1313.

[41] Kokjohn S, Musculus M, Reitz R. Evaluating temperature and fuel stratification for heat-release rate control in a reactivity-controlled compression-ignition engine using optical diagnostics and chemical kinetics modeling. Combustion and Flame, 162 (2015) 2729–2742.

[42] Benajes J, Molina S, Novella R, Amorim R. Study on low temperature combustion for light-duty Diesel engines. Energy and fuels, vol. 24, 355-364, 2010.

[43]Dec J E, Yang Y. Boosted HCCI for high power without engine knock and with ultra-low NOx emissions using conventional gasoline. SAE Int. J. Engines, 2010, 3(1), 750–767.

[44]Musculus MPB, Miles PC, Pickett LM. Conceptual models for partially premixed low-temperature diesel combustion. Progress in Energy and Combustion Science 39 (2013) 246e283.

[45] Pickett LM, Manin J, Genzale CL, Siebers DL, Musculus MPB, Idicheria CA. Relationship between diesel fuel-jet vapor penetration/dispersion and local fuel mixture-fraction. SAE Paper 2011-01-0686 SAE International Journal of Engines 2011;4:764e99.

[46]Siebers DL, Higgins BS. Flame lift-off on direct-injection diesel sprays under quiescent conditions. SAE Paper 2001-01-0530 SAE Transactions 2001; 110(3):400e21.

[47] Prikhodko V, Curran S, Parks J and Wagner R. Effectiveness of Diesel Oxidation Catalyst in Reducing HC and CO Emissions from Reactivity Controlled Compression Ignition. SAE Int. J. Fuels Lubr. 6(2):329-335, 2013, doi:10.4271/2013-01-0515.

Abbreviations

1-D: One-dimensional

ASTM: American Society of Testing and Materials

ATDC: After Top Dead Center

CAD: Crank Angle Degree

CA10: Cranck Angle at 10% mass fraction burned

CA50: Cranck Angle at 50% mass fraction burned

CA90: Cranck Angle at 90% mass fraction burned

CO: Carbon Monoxide

CI: Compression Ignition

DI: Direct Injection

DOC: Diesel Oxidation Catalyst

DPF: Diesel Particulate Filter

EGR: Exhaust Gas Recirculation

EVC: Exhaust Valve Close

EVO: Exhaust Valve Open

EOC: End of Combustion

FSN: Filter Smoke Number

GIE: Gross Indicated Efficiency

HC: Hydro Carbons

HCCI: Homogeneous Charge Compression Ignition

HD: Heavy Duty

HT: Heat Transfer

IVC: Intake Valve Close

IVO: Intake Valve Open

LHV: Lower Heating Value

LTC: Low Temperature Combustion

LTHR: Low Temperature Heat Release

MON: Motor Octane Number

ON: Octane Number

PM: Particulate Matter

PFI: Port Fuel Injection

PER: Premixed Energy Ratio

PPC: Partially Premixed Charge

PRF: Primary Reference Fuel

RCCI: Reactivity Controlled Compression Ignition

RON: Research Octane Number

RoHR: Rate of Heat Release

RI: Ringing Intensity

SOC: Start of Combustion

SOI: Start of Injection

WHSC: World Harmonized Stationary Cycle

Engine type	Single cylinder, 4 St cycle, DI
Bore x Stroke [mm]	123 x 152
Connecting rod length [mm]	225
Displacement [L]	1.806
Geometric compression ratio [-]	14.4:1
Bowl Type	Open crater
Number of Valves	4
IVO	375 CAD ATDC
IVC	535 CAD ATDC
EVO	147 CAD ATDC
EVC	347 CAD ATDC

Table 1. Single cylinder engine specifications.

Variable measured	Device	Manufacturer / model	Accuracy
In-cylinder pressure	Piezoelectric transducer	Kistler / 6125B	±1.25 bar
Intake/exhaust pressure	Piezorresistive transducers	Kistler / 4045A10	±25 mbar
Temperature in settling chambers and manifolds	Thermocouple	TC direct / type K	±2.5 °C
Crank angle, engine speed	Encoder	AVL / 364	±0.02 CAD
NOx, CO, HC, O_2, CO_2	Gas analyzer	HORIBA / Mexa 7100 DEGR	4%
FSN	Smoke meter	AVL / 415	±0.025 FSN
Gasoline/diesel fuel mass flow	Fuel balances	AVL / 733S	±0.2%
Air mass flow	Air flow meter	Elster / RVG G100	±0.1%

Table 2. Accuracy of the instrumentation used in this work.

Diesel injector		Gasoline injector	
Actuation Type	Solenoid	Injector Style	Saturated
Steady flow rate @ 100 bar [cm^3/s]	28.56	Steady flow rate @ 3 bar [cm^3/s]	980
Number of Holes	7	Included Spray Angle [°]	30
Hole diameter [um]	194	Fuel Pressure [bar]	5.5
Included Spray Angle [°]	142	Start of Injection [CAD aTDC]	385

Table 3. Diesel and gasoline fuel injector characteristics.

	Diesel B7	E10-95	E20-95	E10-98	E85
Density [kg/m^3] (T= 15 °C)	837.9	739	745	755	781
Viscosity [mm^2/s] (T= 40 °C)	2.67	-	-	-	-
RON [-]	-	98.8	99.1	103	108
MON [-]	-	85.2	85.6	90	89
Cetane number [-]	54	-	-	-	-
Oxygen content [% mass]	0.8	3.5	6.6	3.5	29.7
Lower heating value [kJ/kg]	42.61	41.32	40.05	41.29	31.56

Table 4. Physical and chemical properties of the fuels used along the study.

	PER=49%	PER=59%	PER=69%	PER=79%
Diesel B7 [mg]	35	28	21	14
E20-95 [mg]	35	42	49	56
E10-95 [mg]	33.9	40.7	47.5	54.3
E10-98 [mg]	33.9	40.7	47.5	54.3
E85 [mg]	44.4	53.3	62.2	71.1
Total Energy [J]	2893.1	2875.2	2857.3	2839.3

Table 5. Fuel mass per blend as well as the total energy delivered to the cylinder for each premixed energy ratio.

Engine speed [rev/min]	1200
Combustion phasing (CA50) [CAD ATDC]	5
Intake Temperature [°C]	40
Diesel pilot inj. timing [CAD ATDC]	-60
Fuel mass in pilot Diesel inj. [%]	50
Diesel main inj. timing [CAD ATDC]	-30
Diesel injection pressure [bar]	700
Low reactivity fuel inj. timing [CAD ATDC]	385

Table 6. Constant engine settings.

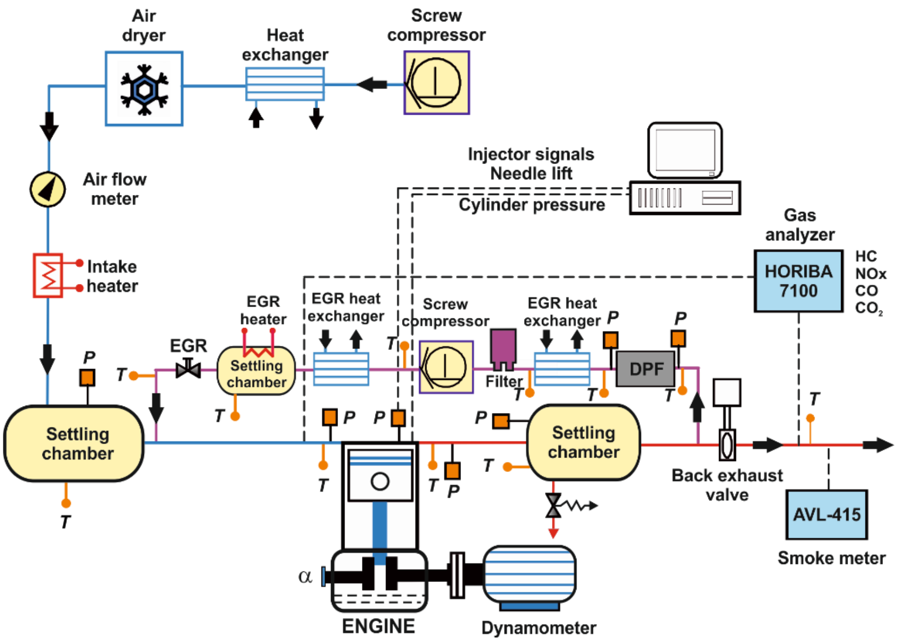

Figure 1. Complete test cell setup

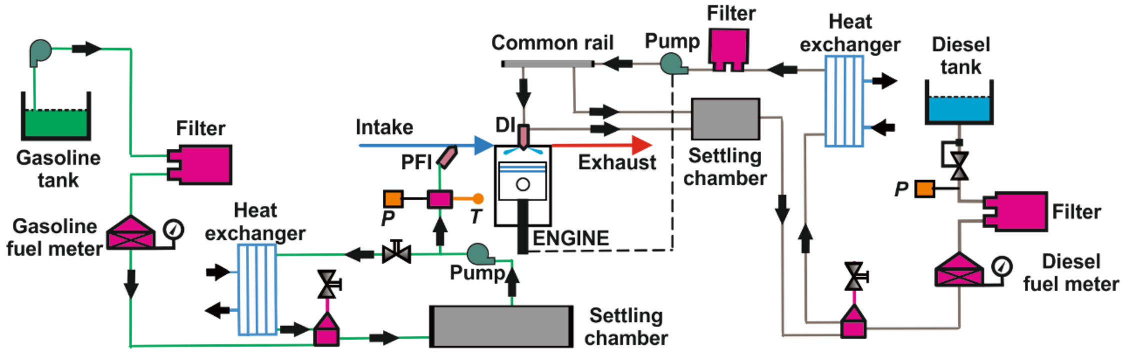

Figure 2. Fuel injection systems scheme

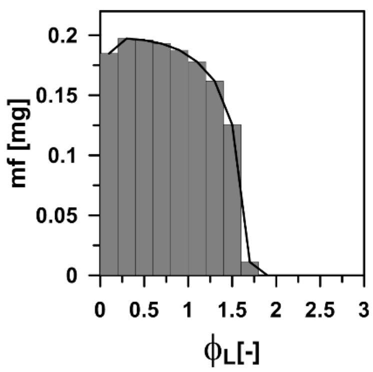

Figure 3. Histogram of the high reactivity fuel mass distribution mixed to different equivalence ratios at experimental SoC

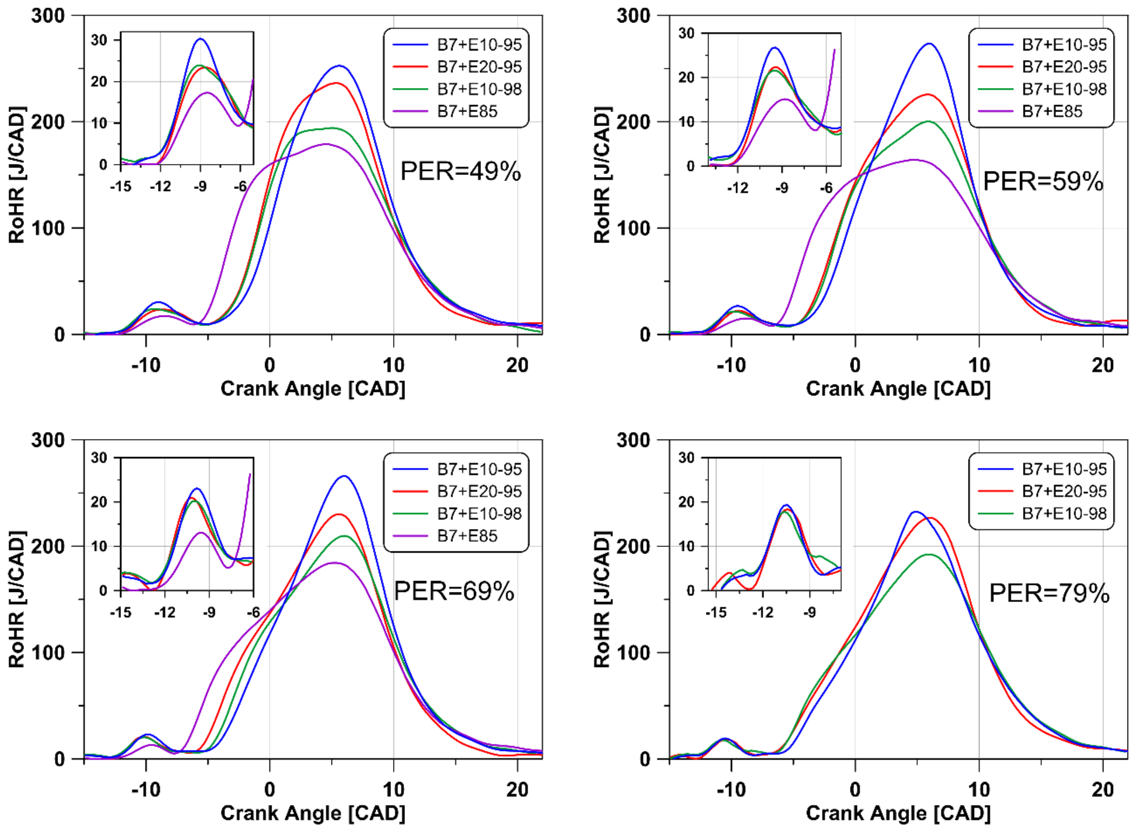

Figure 4. RoHR traces for the different premixed energy ratios and blends

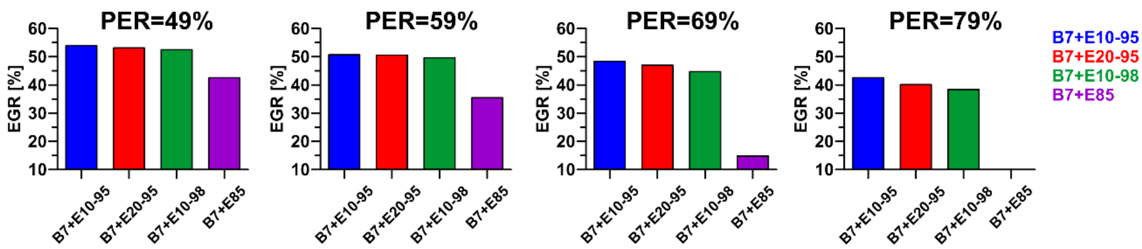

Figure 5. EGR rate for the different premixed energy ratios and blends

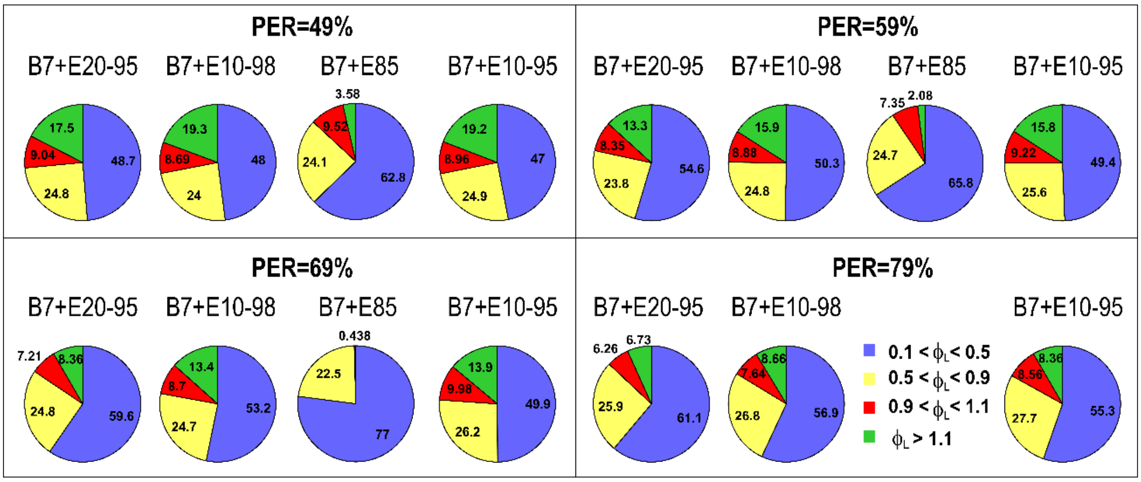

Figure 6. High reactivity fuel mass distribution mixed to different ϕ at experimental SoC for the different premixed energy ratios and blends

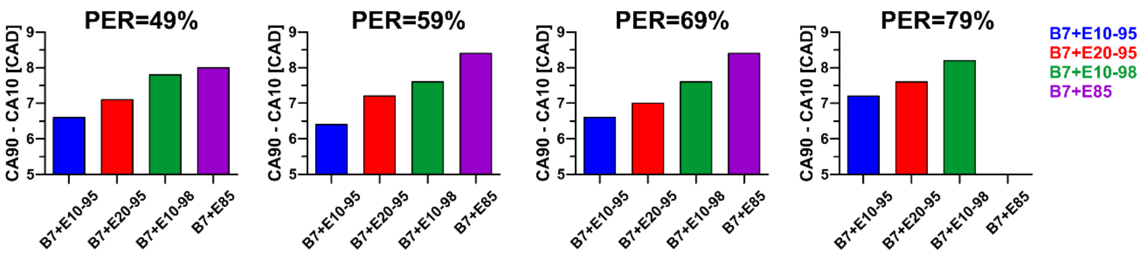

Figure 7. Combustion duration (CA90-CA10) for the different premixed energy ratios and blends

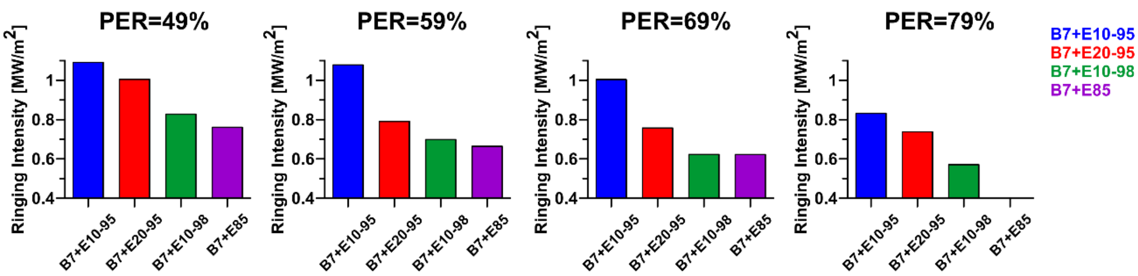

Figure 8. Ringing intensity for the different premixed energy ratios and blends

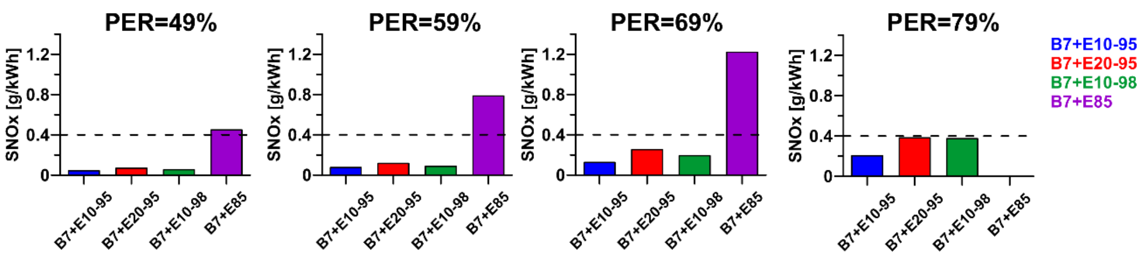

Figure 9. NOx emissions for the different premixed energy ratios and blends

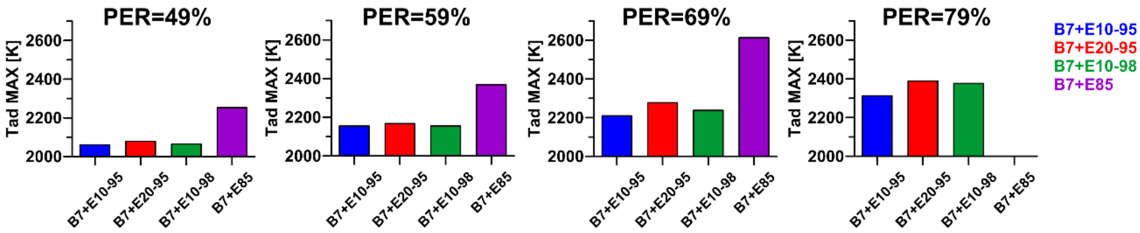

Figure 10. Maximum adiabatic combustion temperature

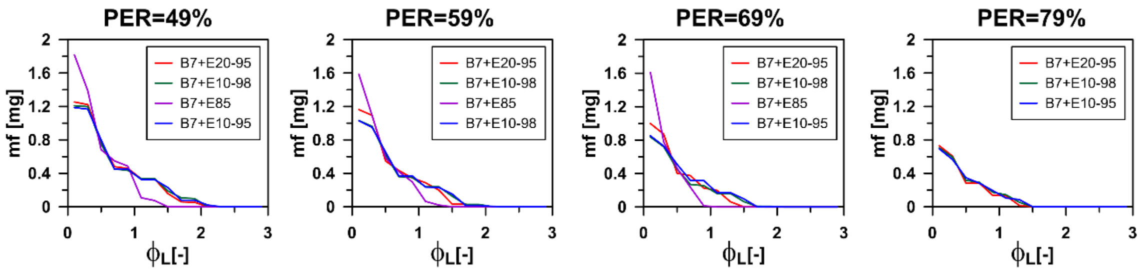

Figure 11. Mass distribution mixed up to different equivalence ratios at experimental SoC for the different premixed energy ratios and blends

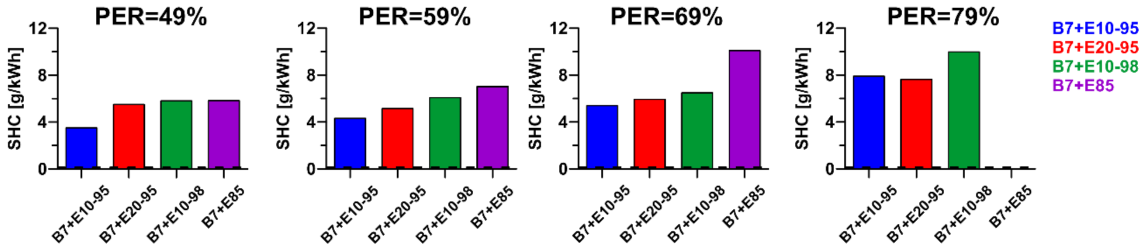

Figure 12. HC emissions for the different premixed energy ratios and blends

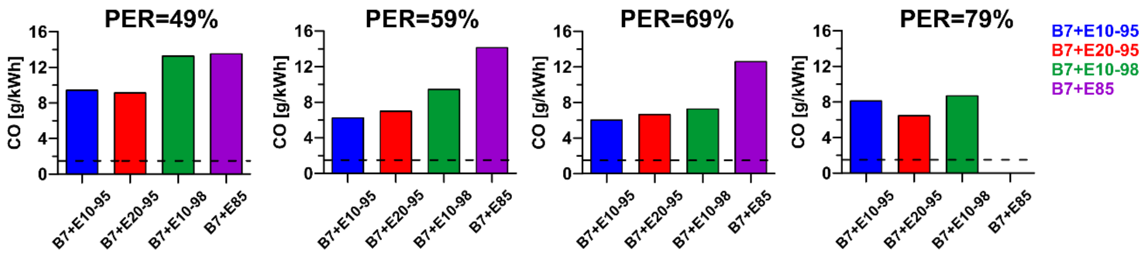

Figure 13. CO emissions for the different premixed energy ratios and blends

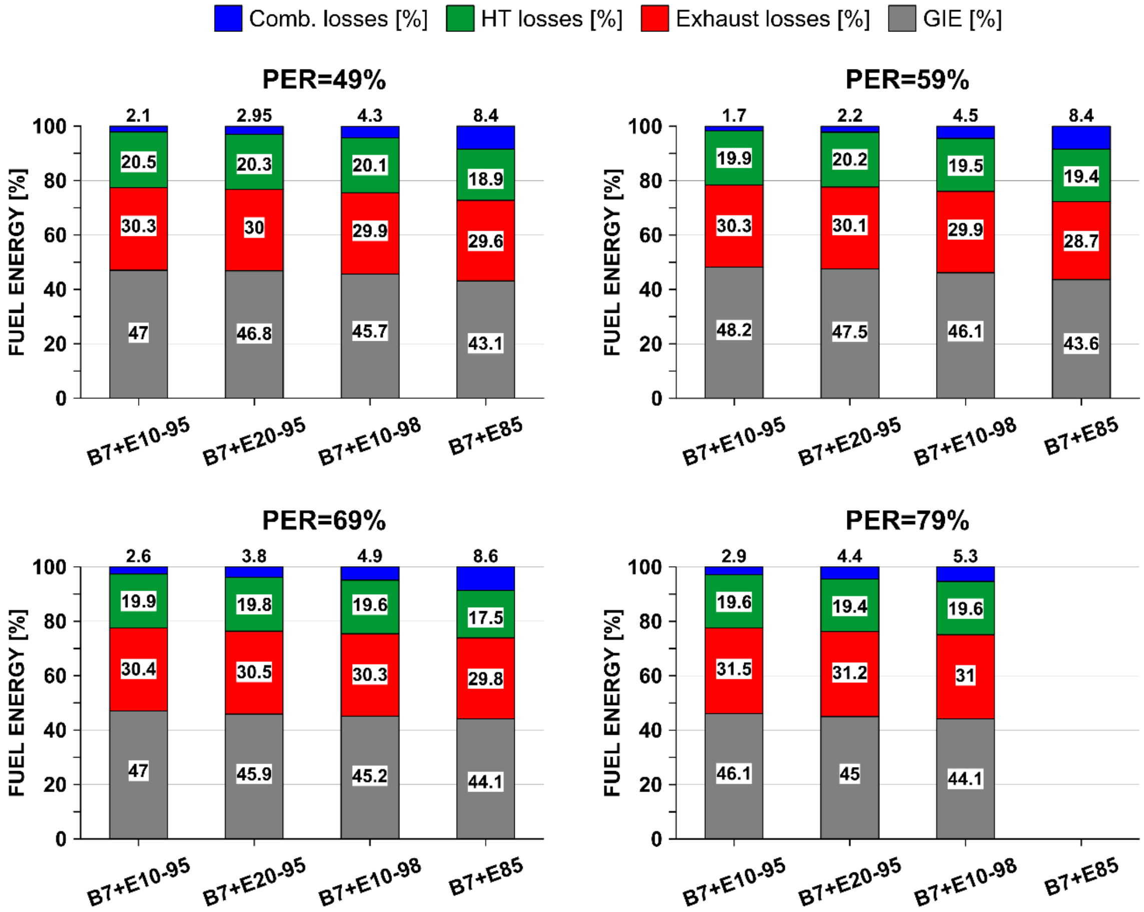

Figure 14. Gross indicated efficiency (GIE), heat transfer losses, exhaust losses and combustion losses as a percentage of the fuel energy for the different premixed energy ratios and blends.